Environmental Science Water Research & Technology

PAPER

View Article Online
View Journal

Published on 28 December 2021. Downloaded by Rice University on 1/19/2022 7:49:35 PM.

Check for updates

Cite this: DOI: 10.1039/d1ew00717c

Modeling SARS-CoV-2 RNA degradation in small and large sewersheds†

Camille McCall,[a] Zheng N. Fang,[b] Dongfeng Li,[b] Andrew J. Czubai,[b] Andrew Juan,[a] Zachary W. LaTurner,[a] Katherine Ensor,[c] Loren Hopkins,[cd] Philip B. Bedient[a] and Lauren B. Stadler*[a]

Received 1st October 2021,
Accepted 22nd December 2021

DOI: 10.1039/d1ew00717c

rsc.li/es-water

Wastewater-based epidemiology has played a significant role in monitoring the COVID-19 pandemic, yet little is known about degradation of SARS-CoV-2 in sewer networks. Here, we used advanced sewershed modeling software to simulate SARS-CoV-2 RNA degradation in sewersheds across Houston, TX under various temperatures and decay rates. Moreover, a novel metric, population times travel time (*PT*), was proposed to identify localities with a greater likelihood of undetected COVID-19 outbreaks and to aid in the placement of upstream samplers. Findings suggest that travel time has a greater influence on RNA degradation across the sewershed as compared to temperature. SARS-CoV-2 RNA degradation at median travel times was approximately two times greater in 20 °C wastewater between the small sewershed, Chocolate Bayou, and the larger sewershed, 69th Street. Lastly, placement of upstream samplers according to the *PT* metric can provide a more representative snapshot of disease incidence in large sewersheds. This study helps to elucidate discrepancies between SARS-CoV-2 viral load in wastewater and clinical incidence of COVID-19. Incorporating travel time and SARS-CoV-2 RNA decay can improve wastewater surveillance efforts.

Water impact

Microbial decay in sewer collection systems poses a significant challenge for wastewater-based epidemiology (WBE) for COVID-19 among other diseases. This work facilitates the understanding of SARS-CoV-2 decay in small and large sewersheds and under various wastewater temperatures. With this information we proposed a novel approach to designing a reliable and sustainable sampling infrastructure for WBE.

1. Introduction

Municipal wastewater treatment plants collect untreated wastewater from communities ranging from hundreds to millions of inhabitants per day within a given sewershed. This wastewater can be scrutinized to obtain critical insights into biological and chemical markers that are reflective of community health within the serviced population, an approach known as wastewater-based epidemiology (WBE).

In WBE, untreated wastewater is considered analogous to a population-wide urine and stool sample. This representative sample can be used to evaluate community health and the prevalence of certain diseases by directly measuring markers of concern. Viral monitoring in wastewater has gained much attention considering that viruses do not replicate independent of a host cell and are persistent in the environment. Several viral pathogens including hepatitis A virus, hepatitis E virus, norovirus, sapovirus, astrovirus, and poliovirus have been monitored in wastewater for community health tracking.[1–5]

Recently, WBE has been recognized as a promising tool for tracking SARS-CoV-2, the causative agent of coronavirus disease 2019 (COVID-19). SARS-CoV-2 is an enveloped positive-sense RNA virus belonging to the *Coronaviridae* family. Although the primary transmission route of SARS-CoV-2 is *via* respiratory droplets, evidence of fecal shedding of SARS-CoV-2 in infected individuals has led to the global attention of WBE in the ongoing fight against COVID-19.[6] Several studies have highlighted the potential for viral signals to precede clinical cases and capture the extent of asymptomatic individuals that are not reported in health care facilities.[7–10]

[a] *Department of Civil and Environmental Engineering, Rice University, 6100 Main Street, MS-519, Houston, TX, 77005, USA. E-mail: lauren.stadler@rice.edu*
[b] *Department of Civil Engineering, The University of Texas at Arlington, Arlington, TX, 76019, USA*
[c] *Department of Statistics, Rice University, Houston, TX, 77005, USA*
[d] *Houston Health Department, 8000 N. Stadium Dr., Houston, TX, 77054, USA*
† Electronic supplementary information (ESI) available. See DOI: 10.1039/d1ew00717c

Published on 28 December 2021. Downloaded by Rice University on 1/19/2022 7:49:35 PM.

Generally, evidence supports the utility of WBE as a public health and environmental tracking tool for viral disease outbreaks. Still, in some cases discrepancies exist between viral signal in wastewater and disease prevalence, specifically with SARS-CoV-2.[11]

Viral measurements from wastewater alone may not be sufficient for disease tracking. Considerations such as the environmental matrix, sampling regimen, sewer collection system, viral stability, and disease characteristics are critical aspects to establishing correlations between viral signal and disease incidence in the community.[12] Among these critical considerations is the stability of the virus and its genetic material in the sewershed. Microbial degradation plays a significant role in determining what proportion of RNA shed in feces gets captured at the outfall of a wastewater treatment plant (WWTP). To date, few studies have investigated RNA degradation of SARS-CoV-2 in wastewater.[13–16]

In two of the studies, temperature had a significant influence on variations between first-order decay rates.[11,13] Temperature was also found to have a greater impact on RNA degradation than the sample matrix.[15] Despite the agreement on the importance of temperature between the two studies, Weidhaas *et al.*, 2021 (ref. 13) obtained a significantly higher decay constant (4.32 day^{-1}) at 35 °C than Ahmed *et al.*, 2020 (ref. 15) (0.29 day^{-1}) at 37 °C for similar gene targets. This indicates that there are other factors that have a notable influence on RNA degradation such as sample preparation or wastewater composition. A recent study demonstrated that the abundance of the SARS-CoV-2 N1 marker is associated with total organic carbon and pH.[17] Furthermore, Bivins *et al.* 2020 (ref. 14) evaluated changes in decay constants when the starting viral titer was low as compared to high titers. Low titers (10^3 TCID$_{50}$ per mL) obtained a decay constant of 0.09 day^{-1} at 20 °C which was significantly lower than that of the high titer (10^5 TCID$_{50}$ per mL) at the same temperature, 0.67 day^{-1}.

From these studies it is evident that further work is needed to understand degradation of SARS-CoV-2 under various conditions. Moreover, only one study to date has explored degradation of SARS-CoV-2 in sewer systems using a first-order decay rate derived from a study on the infectivity of various coronaviruses in wastewater after 21 days.[16,18] The authors found that larger sewersheds further confound the effects of temperature on degradation. Indeed, it is expected that longer travel times will create notable discrepancies between viral concentration and COVID cases in communities. Furthermore, since upstream sampling provides high spatial resolution and is more representative of the sampled population,[16,19] the placement of wastewater samplers in sewersheds remains an ongoing area of interest.[20,21] Yet, to our knowledge, no quantitative approaches for selecting upstream sampling locations to capture outbreaks and minimize degradation of SARS-CoV-2 RNA have been proposed.

Upstream sampling refers to sampling within the sewer system from locations such as manholes, as compared to sampling at the influent of a WWTP (downstream sampling). Several studies have implemented upstream sampling for monitoring COVID-19 outbreaks in hospitals,[22] universities,[23] and metropolitan neighborhoods.[24] There are practical constraints that dictate the selection of upstream sites, namely available resources, accessibility, and safety. Moreover, sampling site selection based on travel time should be considered to further increase the impact of upstream sampling on WBE outcomes.

Interestingly, Haak *et al.* 2022 (ref. 24) found population density to be highly significant when comparing SARS-CoV-2 RNA concentrations in wastewater between different neighborhoods within the same sewershed. Though the effects of population density on SARS-CoV-2 stability in wastewater are not fully understood, population density remains a significant factor in epidemics and can facilitate the rate at which a disease disseminates within a community. A recent study found population density to have a positive effect on the basic reproductive number (R_o) of COVID-19 with R_o increasing by an average of 0.11 when population density doubled.[25] Likewise, a study assessing the effect of several environmental and geographical factors on COVID-19 cases found population density to be the best predictor of cases when looking at 81 provinces in Turkey.[26] Consequently, the higher the population density, the more potential there is for a disease outbreak. Considering its significance, population density can be a critical component for identifying sampling locations based on potential hotspots for rapid disease spread.

Here, we model SARS-CoV-2 RNA degradation in sewersheds across Houston that vary in service population and geographic area based on published and experimentally derived first-order decay rates, wastewater temperature, and sewershed travel times. Finally, we propose a novel metric for determining critical locations for placing upstream samplers to improve SARS-CoV-2 monitoring in wastewater.

2. Materials and methods

2.1. Study area and overview

Houston has 39 sewersheds with a total service area covering approximately 1451 km^2 (358 580 acres). Of those, ten sewersheds were selected for this study based on the availability of sewershed hydraulic models provided by Houston Public Works. The location and characteristics of the selected sewersheds are detailed in Fig. 1 and Table S1,† respectively. Hydraulic modeling was conducted to simulate performance metrics which were then used to compute travel times for each sewershed. Multiple SARS-CoV-2 decay rates based on published and experimental studies were then used with the computed travel times to estimate viral RNA degradation in the sewersheds.

2.2. Sewershed modeling

Hydraulic modeling of sewersheds in this study was accomplished using the Infoworks ICM software (ICM stands

 This journal is © The Royal Society of Chemistry 2022

Published on 28 December 2021. Downloaded by Rice University on 1/19/2022 7:49:35 PM.

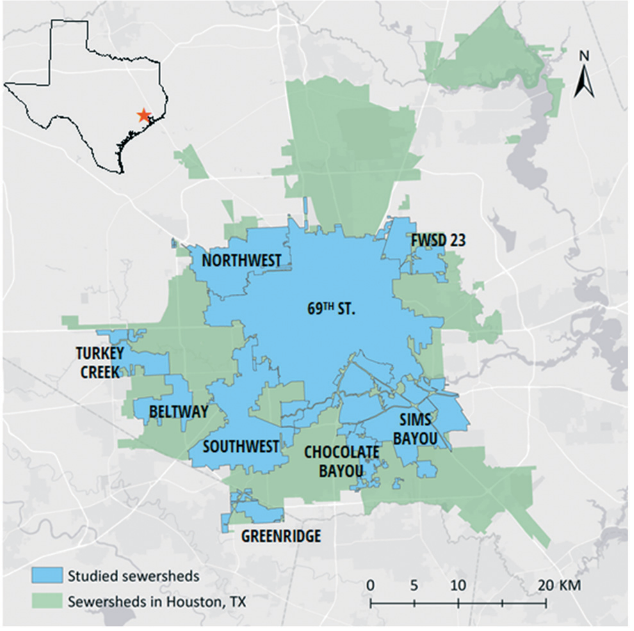

Fig. 1 Ten selected wastewater treatment plant service areas (sewersheds) are shown in blue. Sims Bayou has overlapping service areas recognized as Sims Bayou North and South sewersheds. The remainder of Houston's sewersheds are shown in green.

for integrated catchment modeling). Developed by Innovyze®, Infoworks ICM is a hydrodynamic model capable of simulating the hydrology and hydraulics of aboveground surfaces as well as underground drainage networks based on the conservation of mass and momentum. Due to its robustness and versatility, Infoworks ICM has been used by numerous municipalities, like the City of Houston, for stormwater, flood control infrastructure, and sewer management.

In this study, Infoworks ICM models for ten sewersheds were obtained from the City of Houston Public Works department. Each model represents the wastewater network and service areas for a sewershed. The models were calibrated by Houston Public Works under dry and wet weather conditions. At a minimum, two rainfall events are used for model calibration and one event for verification. A previous study applied a similar approach using an Infoworks ICM model and obtained strong correlations between observed and simulated water levels in a pumping station during a rainfall event.[27] Infoworks ICM provides separate solution models for permeable planes, force mains, pressurized pipes or normal gravity flow. An ICM model consists of a network of links and nodes, in which the links represent pipes or conduits, and the nodes represent manholes or other control structures (*e.g.*, outfall or WWTP). Additionally, the model allows for either one or multiple outfall locations. Based on the connectivity of the nodes and links, service areas that drain to any particular node could be further separated into individual subcatchments. The gradient or slope of the link is calculated using the provided starting and ending invert elevations.

ICM divides each conduit into a number of discrete computational points and regularly-spaced segments with intervals that are 20 times the pipe diameter. Flow, velocity, and other performance metrics are computed in each segment. Inflow can be added to certain nodes as point sources, but in this study, diurnal curves in the form of wastewater profiles with hourly time steps were applied at corresponding subcatchments to represent wet and dry conditions. With specified information of population and *per capita* flow, the wastewater profile can be developed from a calibrated model and is designed to mimic dry weather flow as typically seen during flow monitoring.

2.3. Computing travel time

While various performance metrics such as head, flow, velocity, volume, and water depth are computed by ICM, individual travel times for subcatchments are not. In a typical wastewater system, the conduits are connected to a common outfall, which usually represents the local WWTP. All model networks must have at least one common outfall, but networks are allowed to have multiple outfalls which could represent wet-weather overflows, emergency bypasses, or pump stations to a different wastewater system. Because there is not always a single common outfall, a structured query language (SQL) script was developed to allow users to specify a terminal point. Having terminal points enables travel time to be computed from any subcatchment to the specified points. The user determines the number of iterations for the query, the minimum assumed velocity, and the specific simulation time that the query would run. The query then uses the trace tool, which selects all upstream conduits, nodes, and subcatchments to a specified point and iterates the simulated results to determine a corresponding travel time based on the cumulative conduit length travelled and velocity at the given point. In the case where multiple flow paths exist, the query assumes that wastewater would always travel on the shortest path, therefore computing the shortest travel time from the point of entry to the terminal point. Lastly, the computed travel times for the entire model network were then exported into GIS for further analysis.

2.4. Identifying decay rate studies

A literature search was conducted in October 2020 and again in February 2021 using Web of Science and Google Scholar databases to identify studies with first-order degradation rates for SARS-CoV-2 RNA. SARS-CoV-2 was used as a keyword paired with one or more of the following: wastewater, degradation, decay, sewershed, persistence, fate, and survivability. The criteria for inclusion were (1) peer-viewed journal articles (excluded reviews, metadata, pre-prints, editorial material), (2) a focus on SARS-CoV-2 in untreated wastewater samples or simulated untreated wastewater, (3) includes at least one original, experimentally determined decay rate for SARS-CoV-2 RNA.

Published on 28 December 2021. Downloaded by Rice University on 1/19/2022 7:49:35 PM.

2.5. Decay of SARS-CoV-2 RNA in sewage

Along with experimentally determined decay rates of SARS-CoV-2 from published literature, decay rates were also generated. To determine decay rates for SARS-CoV-2 RNA, roughly 1 gallon of wastewater influent was collected from a 24-hour composite sampler and transported on ice to Houston Public Works central processing laboratory. Approximately 500 mL of wastewater was collected in triplicate, stored in Nalgene bottles, and transported on ice to Rice University. The 500 mL bottles were weighed to accurately determine the volume of wastewater in each bottle. Next, each sample was poured into a sterilized 1 L Erlenmeyer flask containing a stir bar. Flasks were loosely capped with aluminum foil to prevent evaporation and placed on a stir plate at the lowest possible setting to maintain a heterogeneous mixture.

A 50 mL sample was immediately collected from each flask and concentrated *via* the HA filtration method with beat beating as previously described here.[28] HA filters were stored at −80 °C. Wastewater from each flask was collected, concentrated, and stored *via* this method every 24 hours for the next 6 days. All wastewater samples were incubated at room temperature (~20 °C) in a biosafety cabinet. After the 6 days, all stored samples were simultaneously extracted using the Qiagen Allprep Powerviral DNA/RNA kit (Qiagen) with some modifications to the manufacturer's protocol. Briefly, 7 μL of β-mercaptoethanol and 693 μL of PM1 solution were added to each bead tube containing the sample filters. Samples were then bead beaten at 3500 rpm in a Mini-Beadbeater 24 (BioSpec) for 1 min, cooled on ice for 2 min, and bead beaten once more for 1 min. Following bead beating, samples were centrifuged at 17 000*g* for 2 min. Roughly 450 μL of sample lysate was extracted from each bead tube and transferred to a QIAcube Connect (Qiagen) for automated extraction. Samples were eluted in 50 μL of nuclease-free water, stored at −20 °C, and processed within 24 hours.

SARS-CoV-2 N1 and N2 gene targets were quantified in wastewater extracts using a previously described method.[28] In short, a duplex reverse transcriptase digital droplet PCR (RT-ddPCR) was carried out using the One-Step RT-ddPCR Advanced kit for probes (Bio-Rad) on a QX200 AutoDG Droplet Digital PCR System (Bio-Rad) according the manufacturer's recommendations. Ten microliters of RNA extract, no template control, or positive control was transferred to a 12 μL reaction mix containing final concentrations of 900 nmol of each primer and 250 nmol for each probe. All reactions were performed in triplicate with thermocycling conditions detailed here.[28] Samples were then read on a QX200 Droplet Reader (Bio-Rad) and analyzed using the QuantaSoft v1.7.4 software. The limit of quantification (LOQ) was previously determined as 0.767 gene copies per μL of RNA according to a threshold of 3 positive droplets per 10 000 total droplets as recommended by the manufacturer. A linear regression analysis was performed in R[29] to determine the decay rates for each target. Concentrations of SARS-CoV-2 were log-transformed to satisfy the assumptions of normality according to a visual inspection of the quantile–quantile (Q–Q) plots.

2.6. Estimation of SARS-CoV-2 RNA degradation in sewersheds based on first-order decay

To the best of our knowledge, all experimentally-derived published decay rates for SARS-CoV-2 were included in this study. A temperature of 20 °C was used to compare the influence of each decay rate on the proportion of virus loss in select sewersheds across studies. The following formula is an approximation of the Arrhenius equation used to determine the dependence of first-order rates on temperature:[16,30,31]

$$\frac{k_2}{k_1} = {Q_{10}}^{(T_2 - T_1)/10} \tag{1}$$

where Q_{10} is the temperature coefficient, k_1 and k_2 are the lower and upper decay rate constants, respectively, and T_1 and T_2 are the temperatures in Celsius for the upper and lower rate constants, respectively. The temperature coefficient Q_{10} is the factor by which a rate changes given a ten degree increase in temperature and is usually between 2 and 3 for biological systems.[31,32]

Eqn (1) was used to estimate the decay rate at 20 °C for the Weidhaas *et al.*, 2021 (ref. 13) study, using the decay rates measured at 10 and 35 °C. The temperature-dependent linear regression equation reported by the authors was used to determine the decay rate of SARS-CoV-2 RNA at 20 °C for Ahmed *et al.*, 2020.[15]

The degradation of SARS-CoV-2 in the sewershed over time is expected to follow exponential decay as expressed in eqn (2) where $C(t)$ is the concentration of SARS-CoV-2 after time t, C_0 is the initial concentration of SARS-CoV-2 released in the wastewater, and k is the first order decay rate.

$$\frac{C(t)}{C_0} = \mathrm{e}^{-kt} \tag{2}$$

Assuming an initial viral RNA proportion of 1 or 100%, eqn (2) was substituted into eqn (3) to estimate the proportion of SARS-CoV-2 RNA loss (L) eqn (4) or remaining (R) eqn (5) at a given time within the sewershed.

$$\text{Proportion degraded} = 1 - \frac{C(t)}{C_0} \tag{3}$$

$$L = 1 - \mathrm{e}^{-kt} \tag{4}$$

$$R = 1 - L \tag{5}$$

The half-life $t_{\frac{1}{2}}$ and t_{90} (the time for viral load to decrease by one log unit) for each decay rate k were obtained from the published work or derived from the following formulas, respectively:

Published on 28 December 2021. Downloaded by Rice University on 1/19/2022 7:49:35 PM.

$$t_{\frac{1}{2}} = \frac{\ln(2)}{k} \tag{6}$$

$$t_{90} = \frac{-\ln(0.1)}{k} \tag{7}$$

2.7. *PT* metric for identifying hotspots

Aside from using travel time isochrones to determine the spatial distribution of viral RNA signal, they could also be used in conjunction with population density information to help identify potential viral hotspot areas. In this study, a normalized population times travel time (*PT*) metric is introduced to identify critical locations for placing upstream samplers. Normalized *PT* maps for the 69th Street sewershed were generated by multiplying population density information (*P*) in each sub-sewershed area by their corresponding travel times (*T*), and then normalized by the maximum *PT* value computed for the 69th Street and Chocolate Bayou sewersheds. The resulting normalized *PT* maps have values that range from 0 (0%) to 1 (100%). Areas with low *PT* values indicate a low likelihood of an undetected outbreak, due to low population density, short travel times, or both. Conversely, areas with high *PT* values imply a higher likelihood of undetected outbreaks. This is especially true for areas with the highest *PT* values (*i.e.*, at or close to 100%), signifying that those areas have both high population density and long travel times.

3. Results and discussion

3.1. Impact of weather conditions on wastewater travel time in sewersheds

To assess the impact of wet weather on travel times, the ICM model was used to compute travel times under wet and dry conditions for each sewershed (Fig. 2). Travel times under dry weather conditions were generally higher than wet conditions. The 69th Street and Chocolate Bayou sewersheds were used for further analysis due to the differences in characteristics, and because they represented the sewersheds with the largest and smallest service areas studied, respectively.

Median dry weather travel times for 69th Street and Chocolate Bayou were 523 min (s.d. = 217.58 min) and 220 min (s.d. = 152.12 min) with a comparable maximum dry weather travel time of 1207 min and 1123 min, respectively (Fig. 3).

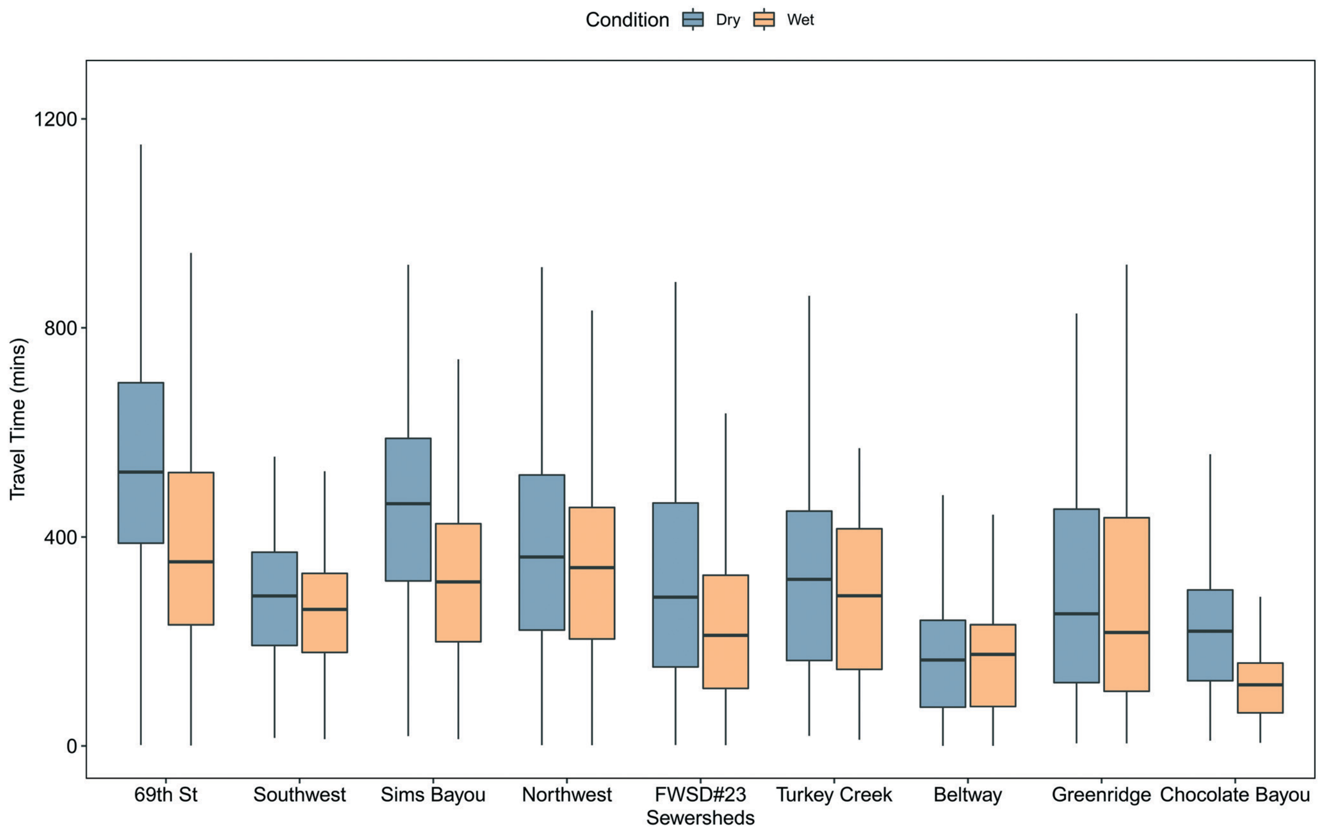

Fig. 2 Boxplot of travel times for select sewersheds under dry and wet weather conditions. Horizontal lines represent the median travel time. Lower and upper whiskers represent the 25th and 75th percentiles, respectively.

Published on 28 December 2021. Downloaded by Rice University on 1/19/2022 7:49:35 PM.

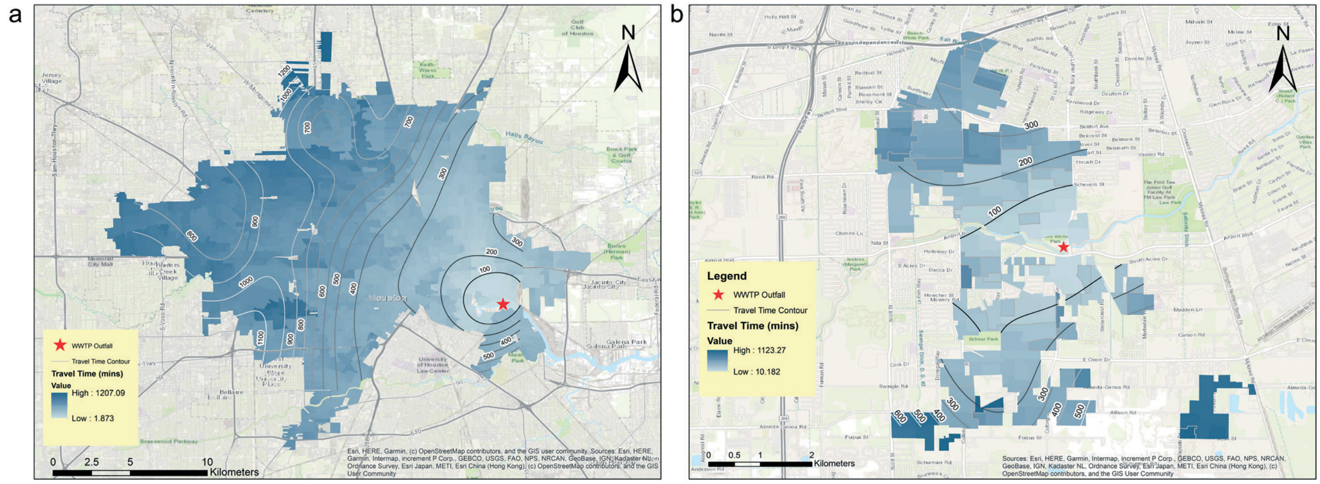

Fig. 3 Heat map displaying travel time for 69th Street (a) and Chocolate Bayou (b). Numbers indicate travel time isochrones in minutes from the WWTP outfall (indicated with a red star).

3.2. Impact of decay rate and temperature on SARS-CoV-2 RNA in transit to wastewater treatment plant

We determined the decay rates of SARS-CoV-2 N1 and N2 at 20 °C using wastewater collected from a sewershed in Houston to compare values using a Houston-specific wastewater to previously published decay rates. After the fourth day of incubation, unclear concentration dynamics occurred wherein the concentration of all targets slightly increased. Due to uncertainty in the cause of this behavior, only the first few days were considered in the regression analysis. Degradation of N1 and N2 showed similar behavior with decay rates of 0.84 day^{-1} and 0.82 day^{-1}, respectively. Table S3† displays the linear regression parameters for each gene. A summary of the ddPCR droplet statistics is detailed in Table S2.† Our experimentally-determined decay rates were within the range of published rates (Table 1). Decay rates listed in Table 1 were used to evaluate the impact of decay rate and temperature on viral RNA degradation in Houston sewersheds.

There were significant differences in how the decay rates in Table 1 were determined, which may explain the wide range of reported rates. Weidhaas *et al.* 2021 (ref. 13) obtained the fastest decay rates compared to studies considered with a rate of (1.75 day^{-1}) at 20 °C. The authors measured SARS-CoV-2 RNA in wastewater samples obtained from two different treatment plants immediately after collection. These initial concentrations were then compared to concentrations measured in replicate samples incubated at 4, 10, and 35 °C for 1 to 22 hours. Ahmed *et al.*, 2020 (ref. 15) spiked SARS-CoV-2-negative wastewater samples with RNA extracted from gamma-irradiated SARS-CoV-2 hCoV-19/Australia/VIC01/2020 isolate and incubated them at 4, 15, 25, and 37 °C over the course of 33 days in which RNA concentrations from those samples were measures every few days.

Decay rates from Bivins *et al.*, 2020 (ref. 14) were the most congruent with results from our lab except under low titer conditions (starting concentration of 10^3 $TCID_{50}$ per mL) (data not shown). The decay rate under low titer conditions was significantly slower than all other reported decay rates listed here.[14] Here, the authors inoculated non-sterile wastewater with a SARS-CoV-2 isolate from a clinical patient diagnosed with COVID-19 at low titer (10^3 $TCID_{50}$ per mL) and high titer (10^5 $TCID_{50}$ per mL) concentrations. SARS-CoV-2 RNA was extracted and quantified in 20 °C inactivated wastewater samples over the course of 7 days. The decay rate associated with the high titer SARS-CoV-2 concentration was selected from the Bivins *et al.*, 2020 (ref. 14) study because it was more representative of concentrations previously measured in Houston sewersheds. Notably, the fastest reported decay rates from Weidhaas *et al.*, 2021 (ref. 13) and our own experiments were determined in samples that were not spiked with virus. This may have been due to the form of the virus in wastewater samples, which is likely a mixture of intact, protected (enveloped and/or intact capsid) virus, and

Table 1 Summary of reported decay rates, half-lives, and t_{90s} (the time for viral concentration to decrease by one log unit) for SARS-CoV-2 RNA targets in various studies at 20 °C

Duration of experiment (day)	Duration of experiment (h)	Target	Decay rate, k (day^{-1})	Half life, $t_{1/2}$ (day)	t_{90} (day)	Comments	Reference
33	792	N1	0.15	4.78	15.88		Ahmed *et al.* 2020 (ref. 15)
1	24	N1, N2	1.75	0.40	1.31		Weidhaas *et al.* 2021 (ref. 13)
6	144	N1	0.84	0.83	2.74		In lab
7	168	E	0.67	0.99	3.30	High titer	Bivins *et al.* 2020 (ref. 14)

 This journal is © The Royal Society of Chemistry 2022

Published on 28 December 2021. Downloaded by Rice University on 1/19/2022 7:49:35 PM.

degraded unprotected viral RNA. Degraded, unprotected viral RNA will degrade much faster than intact, protected virus.[33] A limited number of studies have discriminated between the forms of SARS-CoV-2 in wastewater and have indicated the presence of both intact virus and free RNA.[33,34] As more knowledge on factors that impact the different forms of virus becomes available, consideration should be taken when estimating or selecting SARS-CoV-2 decay rates for sewershed modeling.

Given the ability to estimate decay rates at various temperatures for values obtained from Ahmed *et al.*, 2020 (ref. 15) and Weidhaas *et al.*, 2021,[13] and because they represented the lowest and highest decay rates reported to date, respectively, these studies were used to evaluate the effect of wastewater temperature (20–30 °C) on RNA degradation over time. As expected, viral RNA degradation increases with increasing travel time. Moreover, travel time has a greater influence on degradation as compared to temperature within the range of travel times estimated for the ten sewersheds considered in this study (Fig. 4). However, it is important to note that the impact of temperature on RNA degradation increases with increasing travel times as displayed in Fig. 4. For example, the difference in the percent of RNA degradation between 20 and 30 °C is 0.6% and 9.8% for Ahmed *et al.*, 2020 (ref. 14 and 15) and Weidhaas *et al.*, 2021,[13] respectively after a travel of 120 min compared to 5.2% and 16% at 1200 min.

Similar findings were reported in a recent study that assessed SARS-CoV-2 RNA in sewersheds in Tempe, Arizona under varying wastewater temperatures.[16] The authors concluded that under high temperature conditions in large sewersheds, viral concentration at outfalls may be less representative of disease incidence as compared to colder temperatures. Wastewater temperatures can fluctuate by as much as 27 °C depending on geographical region and seasonal changes.[35] Therefore, careful consideration of wastewater temperatures can be used to improve disease prevalence estimations and explain discrepancies in correlations between the number of disease cases and virus concentrations.

The percent of SARS-CoV-2 RNA degradation in wastewater traveling from a given geographical location within the 69th Street and Chocolate Bayou sewersheds to their corresponding outfalls at the WWTPs was determined using travel time and decay rates from Table 1. As expected, 69th Street showed greater variability in RNA degradation across the sewershed as compared to Chocolate Bayou. Viral RNA degradation at a median travel time of 523 min for 69th Street were 5.13, 21.60, 26.29, and 47.08% for the 0.145, 0.670, 0.840, and 1.752 day^{-1} decay rates, respectively. Chocolate Bayou obtained median percent degradations of 2.19, 9.73, 12.04, and 23.48% at a median travel time of 220 min (Fig. 5). Taking into consideration the decay rate obtained from our study, approximately a 25% reduction in viral signal is estimated in the 69th Street sewershed compared to a 12% reduction for Chocolate Bayou.

Decay rates of 0.840, and 1.752 day^{-1} resulted in SARS-CoV-2 RNA degradation of approximately ≥50% when considering travel times between 1190 and 570 min, respectively. Travel time range between 0–1123 min for the Chocolate Bayou sewershed,

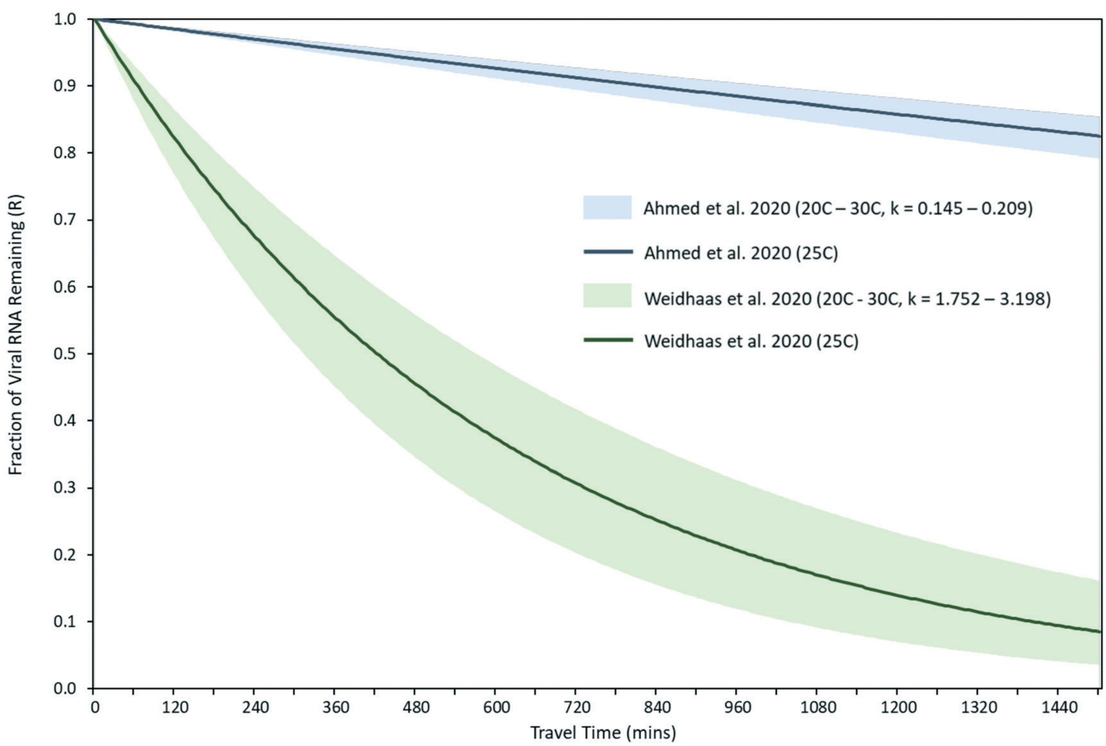

Fig. 4 Effects of temperature, decay rate, and travel time on SARS-CoV-2 RNA degradation.

Published on 28 December 2021. Downloaded by Rice University on 1/19/2022 7:49:35 PM.

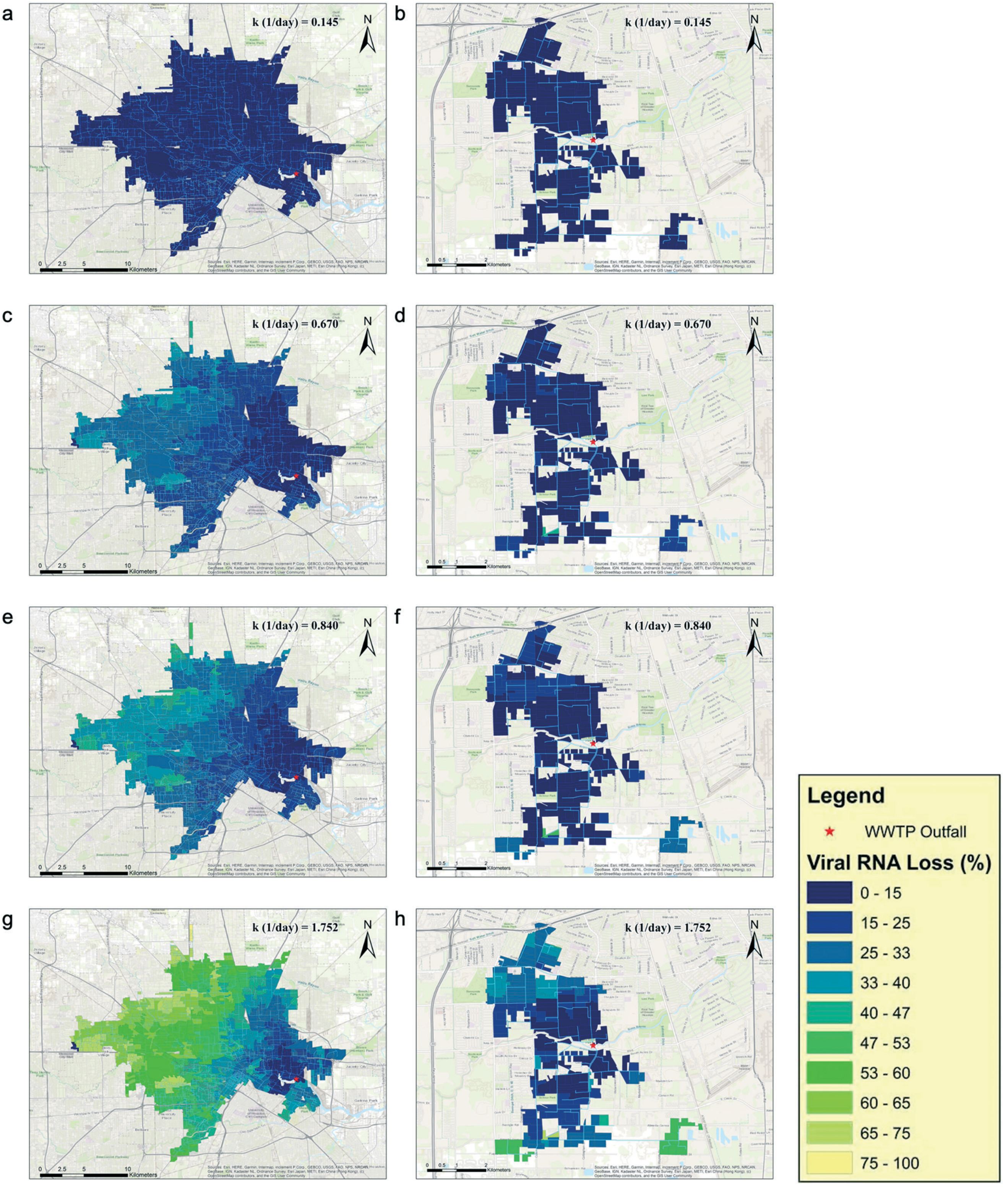

Fig. 5 Geographical heat maps of SARS-CoV-2 RNA degradation for 69th Street (a, c, e and g) and Chocolate Bayou (b, d, f and h) under dry weather conditions and decay rates obtained or estimated from studies listed in Table 1.

thus all regions maintained less than a 50% reduction in viral signal for a decay rate of 0.840 day^{-1}. Despite a greater reduction of viral signal in both sewersheds when considering a virus degradation rate of 1.752 day^{-1}, the fraction of the 69th Street sewershed with ≥50% viral RNA degradation is 49.84% as compared to 2.98% for Chocolate Bayou. Consequently, virus decay is more critical in the 69th Street sewershed due to the number of remote regions.

 This journal is © The Royal Society of Chemistry 2022

Published on 28 December 2021. Downloaded by Rice University on 1/19/2022 7:49:35 PM.

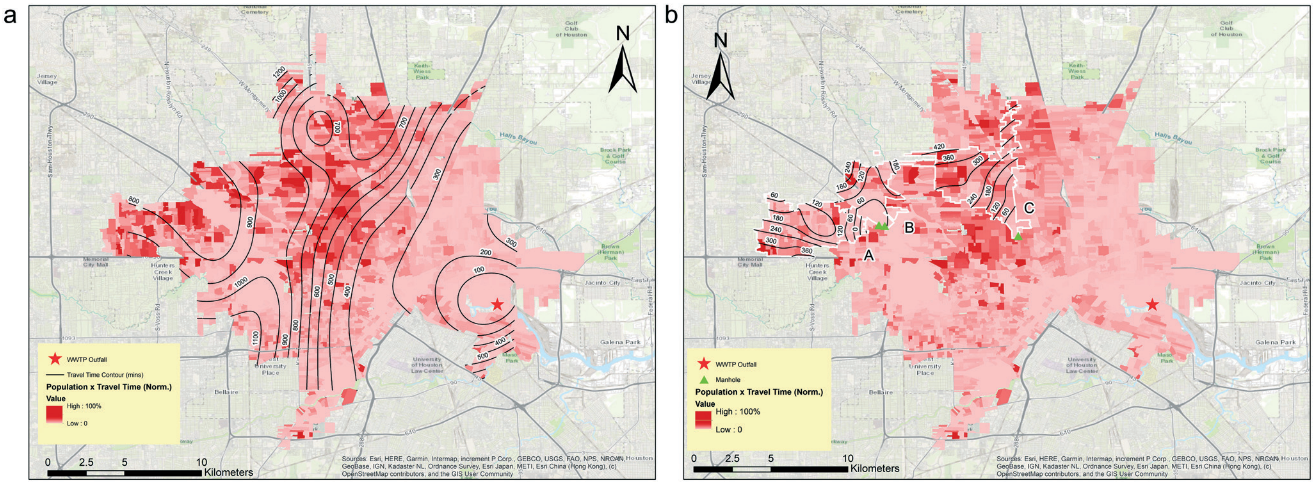

Fig. 6 (a) Display of hotspots in dark red according to normalized *PT* values and (b) placement of samplers and adjusted travel times in sub-catchment zones A, B, and C in the 69th Street sewershed.

3.3. Population *vs.* travel time metric

To account for virus decay across large sewersheds we propose *PT*, a novel metric used to facilitate the placement of upstream samplers and minimize travel times throughout sewersheds. The *PT* metric identifies areas that are at high risk of a wide-spread COVID-19 outbreaks due to population density and the outbreak is less likely to be fully captured in WBE due to prolonged travel times. To evaluate the efficacy of this metric, we estimated *PT* values for all regions within the 69th Street sewershed. Fig. 6a illustrates a *PT* heatmap in the case of downstream sampling only. Hotspots were identified in the northwest-central region of the sewershed.

A second simulation was carried out with three upstream samplers hypothetically placed in hotspots (higher *PT* values), located in the northwest-central region, that were expected to reduce travel times in the sub-sewershed areas and minimize *PT* throughout the sewershed (Fig. 6b). Placement of samplers decreased the median travel time in zones A, B, and C as indicated in Fig. 6b from 865, 840, and 869 min to 154, 129, and 313 min, respectively. Results here indicate that implementation of upstream samplers according to the *PT* metric can significantly reduce the number of hotspots in large sewersheds.

4. Limitations and implications

The scope of this study does not directly take into account other factors that could influence virus degradation such as wastewater composition and microbial predation, which could all further explain or impact conclusions presented here. Since average travel times are approximated from the ICM models, they may not strictly reflect transit of wastewater in the sewersheds, particularly in remote locations and during varying diurnal cycles. Still, findings here indicate that in-sewer decay may be an important factor to consider in WBE and when designing sampling campaigns.

5. Conclusion

A hydraulic modeling approach was applied to 10 Houston sewersheds to estimate travel times and decay of SARS-CoV-2 from source to the WWTP outfall under various temperatures. Travel time generally had a greater impact on viral RNA degradation than wastewater temperature. The largest sewershed showed greater variability in viral RNA degradation due to longer travel times with nearly half of the sewershed losing 50% or more of the viral signal when considering the fastest decay rate. By incorporating a novel *PT* metric for placement of upstream samplers within the largest sewershed, travel times reduced by more than 60%. This reduction is expected to alleviate virus signal loss due to decay and discrepancies between wastewater and clinical cases in wastewater surveillance efforts. This approach can be adopted in various localities to improve sampling infrastructures and public health responses to local and global viral disease outbreaks.

Funding sources

This work was supported by the Houston Health Department and grants from the National Science Foundation (CBET 2029025) and seed funds from Rice University. Zachary W. LaTurner was funded by an Environmental Research & Education Foundation scholarship.

Conflicts of interest

There are no conflicts to declare.

Acknowledgements

A special thanks to Houston Public Works for providing ICM models for selected sewersheds and additional sewershed characteristics where needed. We'd also like to thank the Houston Health Department, and specifically Courtney

View Article Online

Published on 28 December 2021. Downloaded by Rice University on 1/19/2022 7:49:35 PM.

Hundley, Rebecca Schneider, and Lilian Mojica, for providing aggregate travel times for positive COVID-19 cases as needed. We thank Prashant Kalvapalle for his contribution to the wastewater-based epidemiology method development along with the Lauren Stadler and Anthony Maresso lab groups at Rice University and Baylor College of Medicine for their assistance with wastewater sample collection, processing, and analysis.

References

1 M. Bisseux, J. Colombet, A. Mirand, A. M. Roque-Afonso, F. Abravanel and J. Izopet, *et al.* Monitoring human enteric viruses in wastewater and relevance to infections encountered in the clinical setting: A one-year experiment in central France, 2014 to 2015, *Eurosurveillance*, 2018, **23**(7), 1–11.

2 A. F. Brouwer, J. N. S. Eisenberg, C. D. Pomeroy, L. M. Shulman, M. Hindiyeh and Y. Manor, *et al.*, Epidemiology of the silent polio outbreak in Rahat, Israel, based on modeling of environmental surveillance data, *Proc. Natl. Acad. Sci. U. S. A.*, 2018, **115**(45), E10625–E10633.

3 A. H. Kamel, M. A. Ali, H. G. El-Nady, S. Aho, P. Pothier and G. Belliot, Evidence of the co-circulation of enteric viruses in sewage and in the population of Greater Cairo, *J. Appl. Microbiol.*, 2010, **108**(5), 1620–1629.

4 P. Kokkinos, P. Ziros, D. Meri, S. Filippidou, S. Kolla and A. Galanis, *et al.*, Environmental surveillance. An additional/alternative approach for virological surveillance in Greece?, *Int. J. Environ. Res. Public Health*, 2011, **8**(6), 1914–1922.

5 G. la Rosa, S. della Libera, M. Iaconelli, A. R. Ciccaglione, R. Bruni and S. Taffon, *et al.*, Surveillance of hepatitis A virus in urban sewages and comparison with cases notified in the course of an outbreak, Italy 2013, *BMC Infect. Dis.*, 2014, **14**(1), 1–11.

6 S. Parasa, M. Desai, V. Thoguluva Chandrasekar, H. K. Patel, K. F. Kennedy, T. Roesch, M. Spadaccini, M. Colombo, R. Gabbiadini, E. L. A. Artifon, A. Repici and P. Sharma, Prevalence of gastrointestinal symptoms and fecal viral shedding in patients with coronavirus disease 2019: a systematic review and meta-analysis, *JAMA Netw. Open*, 2020, **3**(6), e2011335.

7 G. la Rosa, P. Mancini, G. Bonanno Ferraro, C. Veneri, M. Iaconelli and L. Bonadonna, *et al.*, SARS-CoV-2 has been circulating in northern Italy since December 2019: Evidence from environmental monitoring, *Sci. Total Environ.*, 2021, **750**, 141711.

8 W. Randazzo, P. Truchado, E. Cuevas-Ferrando, P. Simón, A. Allende and G. Sánchez, SARS-CoV-2 RNA in wastewater anticipated COVID-19 occurrence in a low prevalence area, *Water Res.*, 2020, **181**, 115942.

9 L. B. Stadler, K. B. Ensor, J. R. Clark, P. Kalvapalle, Z. W. LaTurner, L. Mojica, A. Terwilliger, Y. Zhuo, P. Ali, V. Avadhanula, R. Bertolusso, T. Crosby, H. Hernandez, M. Hollstein, K. Weesner, D. M. Zong, D. Persse, P. A. Piedra, A. W. Maresso and L. Hopkins, Wastewater Analysis of SARS-CoV-2 as a Predictive Metric of Positivity Rate for a Major Metropolis, *medRxiv*, 2020, DOI: 10.1101/2020.11.04.20226191.

10 F. Wu, J. Zhang, A. Xiao, X. Gu, W. L. Lee and F. Armas, *et al.*, SARS-CoV-2 Titers in Wastewater Are Higher than Expected from Clinically Confirmed Cases, *mSystems*, 2020, **5**(4), e00614-20.

11 W. Ahmed, B. Tscharke, P. M. Bertsch, K. Bibby, A. Bivins and P. Choi, *et al.*, SARS-CoV-2 RNA monitoring in wastewater as a potential early warning system for COVID-19 transmission in the community: A temporal case study, *Sci. Total Environ.*, 2021, **761**, 144216.

12 I. Xagoraraki, Can We Predict Viral Outbreaks Using Wastewater Surveillance?, *J. Environ. Eng.*, 2020, **146**(11), 01820003.

13 J. Weidhaas, Z. T. Aanderud, D. K. Roper, J. VanDerslice, E. B. Gaddis and J. Ostermiller, *et al.*, Correlation of SARS-CoV-2 RNA in wastewater with COVID-19 disease burden in sewersheds, *Sci. Total Environ.*, 2021, **775**, 14579.

14 A. Bivins, J. Greaves, R. Fischer, K. C. Yinda, W. Ahmed and M. Kitajima, *et al.*, Persistence of SARS-CoV-2 in Water and Wastewater, *Environ. Sci. Technol. Lett.*, 2020, **7**(12), 937–942.

15 W. Ahmed, P. M. Bertsch, K. Bibby, E. Haramoto, J. Hewitt, F. Huygens, P. Gyawali, A. Korajkic, S. Riddell, S. P. Sherchan, S. L. Simpson, K. Sirikanchana, E. M. Symonds, R. Verhagen, S. S. Vasan, M. Kitajima and A. Bivins, Decay of SARS-CoV-2 and surrogate murine hepatitis virus RNA in untreated wastewater to inform application in wastewater-based epidemiology, *Environ. Res.*, 2020, **191**, 110092.

16 O. E. Hart and R. U. Halden, Computational analysis of SARS-CoV-2/COVID-19 surveillance by wastewater-based epidemiology locally and globally: Feasibility, economy, opportunities and challenges, *Sci. Total Environ.*, 2020, **730**, 138875.

17 P. Y. Hong, A. T. Rachmadi, D. Mantilla-Calderon, M. Alkahtani, Y. M. Bashawri and H. al Qarni, *et al.*, Estimating the minimum number of SARS-CoV-2 infected cases needed to detect viral RNA in wastewater: To what extent of the outbreak can surveillance of wastewater tell us?, *Environ. Res.*, 2021, **195**, 110748.

18 P. M. Gundy, C. P. Gerba and I. L. Pepper, Survival of Coronaviruses in Water and Wastewater, *Food Environ. Virol.*, 2009, **1**(1), 10–14.

19 M. Matus, C. Duvallet, M. K. Soule, S. M. Kearney, N. Endo, N. Ghaeli, I. Brito, C. Ratti, E. B. Kujawinski and E. J. Alm, 24-hour multi-omics analysis of residential sewage reflects human activity and informs public health, *bioRxiv*, 2019, 728022.

20 R. C. Larson, O. Berman and M. Nourinejad, Sampling manholes to home in on SARS-CoV-2 infections, *PLoS One*, 2020, **15**, e0240007.

21 R. A. Yeager, R. H. Holm, K. Saurabh, J. L. Fuqua, D. Talley, A. Bhatnagar and T. Smith, Wastewater Sample Site Selection to Estimate Geographically-Resolved Community Prevalence of COVID-19: A Sampling Protocol Perspective, *GeoHealth*, 2021, **5**(7), e2021GH000420.

 This journal is © The Royal Society of Chemistry 2022

Published on 28 December 2021. Downloaded by Rice University on 1/19/2022 7:49:35 PM.
22 N. Acosta, M. A. Bautista, J. Hollman, J. McCalder, A. B. Beaudet and L. Man, *et al.*, A multicenter study investigating SARS-CoV-2 in tertiary-care hospital wastewater. viral burden correlates with increasing hospitalized cases as well as hospital-associated transmissions and outbreaks, *Water Res.*, 2021, **201**, 117369.
23 B. W. Schmitz, G. K. Innes, S. M. Prasek, W. Q. Betancourt, E. R. Stark and A. R. Foster, *et al.*, Enumerating asymptomatic COVID-19 cases and estimating SARS-CoV-2 fecal shedding rates via wastewater-based epidemiology, *Sci. Total Environ.*, 2021, **801**, 149794.
24 L. Haak, B. Delic, L. Li, T. Guarin, L. Mazurowski and N. G. Dastjerdi, *et al.*, Spatial and temporal variability and data bias in wastewater surveillance of SARS-CoV-2 in a sewer system, *Sci. Total Environ.*, 2022, **805**, 150390.
25 K. T. L. Sy, L. F. White and B. E. Nichols, Population density and basic reproductive number of COVID-19 across United States counties, *PLoS One*, 2021, **16**(4), e0249271.
26 H. Coşkun, N. Yıldırım and S. Gündüz, The spread of COVID-19 virus through population density and wind in Turkey cities, *Sci. Total Environ.*, 2021, **751**, 141663.
27 H. Q. Peng, Y. Liu, H. W. Wang and L. M. Ma, Assessment of the service performance of drainage system and transformation of pipeline network based on urban combined sewer system model, *Environ. Sci. Pollut. Res.*, 2015, **22**(20), 15712–15721.
28 Z. W. LaTurner, D. M. Zong, P. Kalvapalle, K. R. Gamas, A. Terwilliger and T. Crosby, *et al.*, Evaluating recovery, cost, and throughput of different concentration methods for SARS-CoV-2 wastewater-based epidemiology, *Water Res.*, 2021, **197**, 117043.
29 R Core Team, R: A language and environment for statistical computing, Vienna, Austria, 2020, [cited 2021 Sep 28], Available from: https://www.r-project.org/.
30 R. A. Blaustein, Y. Pachepsky, R. L. Hill, D. R. Shelton and G. Whelan, Escherichia coli survival in waters: Temperature dependence, *Water Res.*, 2013, **47**(2), 569–578.
31 J. Behradek, Temperature Coefficients in Biology, *Biol. Rev.*, 1930, **5**, 30–59.
32 B. A. Reyes, J. S. Pendergast and S. Yamazaki, Mammalian Peripheral Circadian Oscillators Are Temperature Compensated NIH Public Access, *J. Biol. Rhythms*, 2008, **23**(1), 95–98.
33 S. Wurtzer, P. Waldman, A. Ferrier-Rembert, G. Frenois-Veyrat, J. M. Mouchel and M. Boni, *et al.*, Several forms of SARS-CoV-2 RNA can be detected in wastewaters: Implication for wastewater-based epidemiology and risk assessment, *Water Res.*, 2021, **198**, 117183.
34 V. D. Canh, S. Torii, M. Yasui, S. Kyuwa and H. Katayama, Capsid integrity RT-qPCR for the selective detection of intact SARS-CoV-2 in wastewater, *Sci. Total Environ.*, 2021, **791**, 148342.
35 O. E. Hart and R. U. Halden, Modeling wastewater temperature and attenuation of sewage-borne biomarkers globally, *Water Res.*, 2020, **172**, 115473.